DOI: 10.1002/ejic.201000846

Dimorphic Modifications of the Thiocyanato-Bridged Coordination Polymer $[Ni(NCS)_2(pyridazine)(H_2O)_{0.5}]_n$ with Different Magnetic Properties

Mario Wriedt[a] and Christian Näther*[a]

Keywords: Nickel / Thiocyanate ligands / Coordination polymers / Coordination modes / Thermal properties / Magnetic properties

Reaction of nickel(II) thiocyanate with pyridazine under hydrothermal conditions leads to the formation of the hemihydrate $[Ni(NCS)_2(pyridazine)(H_2O)_{0.5}]_n$ (**1I**). The crystal structure was determined by X-ray single-crystal structure analysis. In the crystal structure two types of Ni^{II} cations are found. Both are coordinated by one μ-1,1-NCS- and two μ-1,3-NCS-bridging thiocyanato anions as well as two μ-1,2-bridging pyridazine ligands. The octahedral coordination sphere of Ni1 is completed by one coordinating water molecule and that of Ni2 by one terminal *N*-bonded thiocyanato anion. These building blocks are connected into chains, which are further connected into a 2D polymeric network by strong interchain hydrogen bonding. By thermal decomposition of the precursor compound **1I**, a new anhydrate $[Ni(NCS)_2(pyridazine)]_n$ (**2**) is obtained. On rehydration, this compound transforms into a new polymorphic hemihydrate modification **1II**. Magnetic measurements of both forms show completely different behavior: Whereas modification **1I** shows a long-range antiferromagnetic ordering state at T_N = 5.4 K, modification **1II** only shows Curie–Weiss paramagnetism with weak ferromagnetic interactions.

Introduction

Over the last decades enormous efforts were made in the investigations on the synthesis, structures, and properties of coordination polymers or metal-organic frameworks.[1] Especially compounds with well-defined magnetic properties – mediated by e.g. small anionic linker ligands – are of considerable interest.[2] In this context among others, thiocyanates are promising candidates because they can mediate magnetic exchange interactions and exhibit distinct structural coordination diversity.[3–5] However, on the basis of a research of the Cambridge Structure Database (database version 5.31 with updates of February 2010), considering only the paramagnetic transition metals Mn^{II}, Fe^{II}, Co^{II}, and Ni^{II}, terminal *N*-coordinated thiocyanates are much more frequent (1694 hits) than μ-1,3-NCS (186 hits) and μ-1,1-NCS-bridging (30 hits) coordinations (Figure 1).

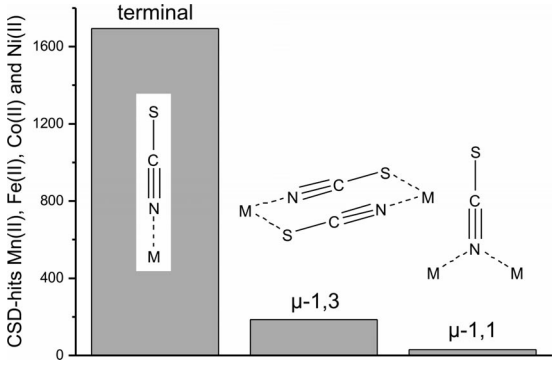

Figure 1. Most common coordination modes of the thiocyanato anion with their frequency distribution in compounds based on the paramagnetic transition metals Mn^{II}, Fe^{II}, Co^{II}, and Ni^{II}: terminal (left), μ-1,3-NCS (middle) and μ-1,1-NCS-bridging (right).

These results suggest that compounds with terminal *N*-coordinating thiocyanato anions are energetically favored. It must be pointed out that thiocyanates in which the most common coordination modes coexist are very rare, and according to the CSD no compound exists in which terminal μ-1,3- and μ-1,1-bridging anions are present. In general, the synthesis of compounds with bridging thiocyanato anions is difficult to achieve and those with terminal bonded thiocyanato anions are frequently obtained. This is disappointing, because especially the bridging ones are of high interest since they can mediate magnetic exchange interactions.

Thus, over the last few years we elaborate an alternative and elegant approach for the discovering and phase-pure synthesis of new coordination polymers with bridging small-sized anions, in which ligand-rich precursor compounds with additional neutral coligands are heated (ligand-rich in the sense of rich in coligands).[6–14] In most cases the coligands are stepwise removed, which leads to the formation of ligand-deficient intermediates. If the ligand-rich precursors consist of paramagnetic transition

[a] Institut für Anorganische Chemie, Universität zu Kiel, Max-Eyth-Straße 2, 24098 Kiel, Germany
Fax: +49-431-8801520
E-mail: cnaether@ac.uni-kiel.de

Supporting information for this article is available on the WWW under http://dx.doi.org/10.1002/ejic.201000846.

metals and small-sized nonbridging magnetically-active anionic ligands, new ligand-deficient intermediates with more condensed coordination networks are frequently obtained, in which the small-sized ligands bridge the metal centers. This structural transformation is accompanied by a dramatic change in their magnetic properties. Whereas most of the ligand-rich compounds only exhibit Curie–Weiss paramagnetism, cooperative magnetic phenomena, like e.g. ferro- or antiferromagnetism, are frequently observed in the ligand-deficient intermediates. It must be noted that such ligand-deficient compounds are in most cases not accessible by reaction of their starting materials in solution, but they can always be prepared phase pure by thermal decomposition of their corresponding ligand-rich precursors. In these investigations we showed that a series of new ligand-deficient compounds with cooperative magnetic exchange interactions based on transition metal thiocyanates,[6–11] selenocyanates,[12] formats,[13] or dicyanamides[14] containing different organic spacer ligands like pyrazine,[6,12] pyrimidine,[7] pyridazine,[8,14] or 4,4′-bipyridine[9–11,13] can be prepared by this elegant route.

In this context it must be mentioned that the removal of coordinated water from hydrates can also lead to the formation of denser structures with modified magnetic properties.[9,10,13,15] However, it must be kept in mind that on rehydration of these anhydrates different polymorphic forms of the hydrates can be obtained.[9] This is of special interest because as a result of their identical composition, all differences in their physical properties can only be traced back to their different structures.

Over the course of systematic investigations we prepared the new compound $[Ni(NCS)_2(pyridazine)(H_2O)_{0.5}]_n$ (**1I**), which represents the first example of a thiocyanato compound in which all three of the most common thiocyanato coordination modes coexist. On heating, the coordinated water molecules are removed leading to the formation of the anhydrate $[Ni(NCS)_2(pyridazine)]_n$ (**2**), which transforms on rehydration into a new hemihydrate modification **1II**. Here we report on these investigations.

Results and Discussion

Crystal Structure

$[Ni(NCS)_2(pyridazine)(H_2O)_{0.5}]_n$ (**1I**) crystallizes in the centrosymmetric triclinic space group $P\bar{1}$ with four formula units in the unit cell (Table 4). The asymmetric unit consists of two nickel(II) cations, two pyridazine ligands, one water molecule, and four thiocyanato anions in general positions. Ni1 is coordinated by one *S*-bonded and two *N*-bonded thiocyanato anions, two pyridazine ligands, and one water molecule in an octahedral coordination mode. Ni2 is coordinated by one *S*-bonded and three *N*-bonded thiocyanato anions and two pyridazine ligands within a slightly distorted octahedron (Figure 2). In the crystal structure the two crystallographic independent nickel(II) cations are connected by two *N*,*N*′-bridging pyridazine ligands forming a six-membered ring. Both nickel(II) cations are further μ-1,1-NCS bridged by a single thiocyanato anion. These building blocks are each connected by four μ-1,3-NCS-bridging thiocyanato anions into chains (Figure 3: top). The octahedral coordination sphere of Ni1 is completed by one coordinating water molecule and that of Ni2 by one terminal *N*-bonded thiocyanato anion. Taking interchain hydrogen bonding into account, the structure of **1I** can be regarded as a two-dimensional layered compound (Table 1; Figure 3: bottom). The NiN_4OS octahedron around Ni1 is markedly distorted with distances ranging between 2.020(3)

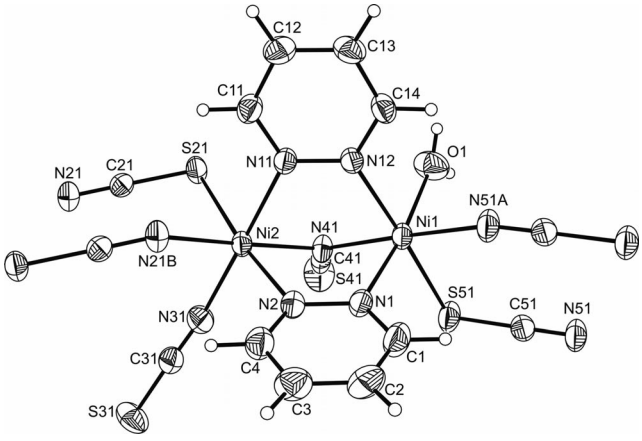

Figure 2. Crystal structure of compound **1I** with a view of the coordination sphere of the Ni^{II} cations with labeling, and the displacement ellipsoid drawn at the 50% probability level. Symmetry codes, A: $-x + 1, -y + 2, -z$; B: $-x, -y + 1, -z + 1$.

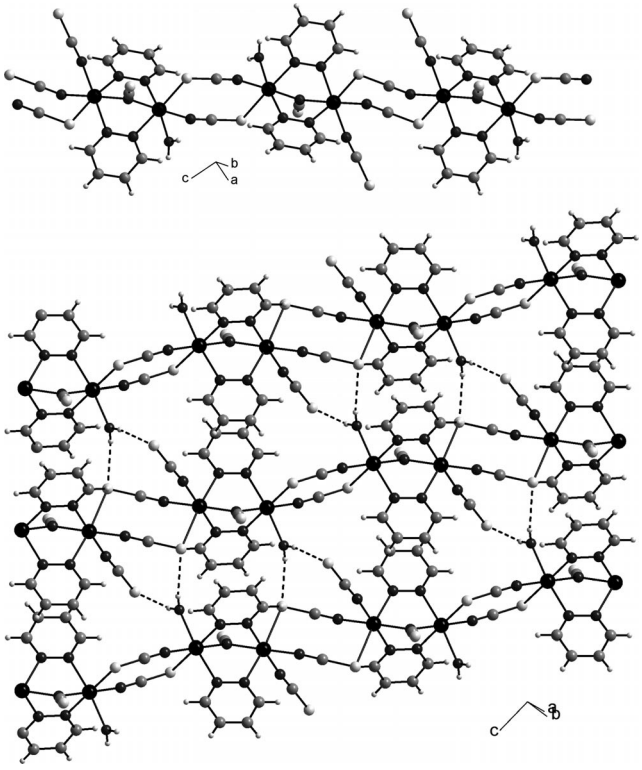

Figure 3. View of a single chain (top) and packing of these chains into layers (bottom) of compound **1I**. Dashed lines indicate O–H···S hydrogen bonding.

and 2.5022(9) Å and angles between 85.11(7)–97.02(7) and 172.25(10)–177.34(11)°. The NiN_5S octahedron around Ni2 is also markedly distorted with distances ranging between 2.030(3) and 2.5350(9) Å and angles between 87.05(10)–94.06(11) and 173.71(8)–178.86(11)° (Table 2). The metal-to-metal separation through the μ-1,1-NCS-bridging thiocyanato anion is 3.310(1) Å with a Ni–N–Ni angle of 105.67(11)° and the metal-to-metal separation through the μ-1,3-NCS-bridging thiocyanato anions is 5.515(1) Å with Ni–N–C angles of 146.4(3) and 162.8(3)° as well as Ni–S–C angles of 100.21(11) and 104.82(11)°. The shortest interlayer metal-to-metal separation is 7.8921(9) Å.

Table 1. O–S···H hydrogen-bond geometry [Å, °] of compound **1I**.

H1–S21	2.661(1)	H2–S31	2.449(9)
O1–S21	3.470(3)	O–S31	3.250(3)
O1–H1–S21	169.6(2)	O1–H2–S31	165.7(2)

Table 2. Selected bond lengths [Å] and angles [°] of compound **1I**.

Ni1–N1	2.106(3)	Ni2–N2	2.116(3)
Ni1–N12	2.096(2)	Ni2–N11	2.101(3)
Ni1–N41	2.070(3)	Ni2–N21B	2.059(3)
Ni1–N51A	2.020(3)	Ni2–N31	2.030(3)
Ni1–S51	2.5022(9)	Ni2–N41	2.083(2)
Ni1–O1	2.110(3)	Ni2–S21	2.5350(9)
N51A-Ni1–N41	177.34(11)	N31–Ni2–N21B	87.60(12)
N51A-Ni1–N12	94.01(10)	N31–Ni2–N41	94.06(11)
N41–Ni1–N12	88.59(10)	N21B-Ni2–N41	178.34(12)
N51A-Ni1–N1	92.39(12)	N31–Ni2–N11	178.86(11)
N41–Ni1–N1	88.35(11)	N21B-Ni2–N11	91.29(11)
N12–Ni1–N1	86.21(10)	N41–Ni2–N11	87.05(10)
N51A-Ni1–O1	90.06(13)	N31–Ni2–N2	93.00(12)
N41–Ni1–O1	89.53(11)	N21B-Ni2–N2	92.50(10)
N12–Ni1–O1	86.28(10)	N41–Ni2–N2	87.42(10)
N1–Ni1–O1	172.25(10)	N11–Ni2–N2	87.26(10)
N51A-Ni1–S51	92.26(8)	N31–Ni2–S21	92.20(9)
N41–Ni1–S51	85.11(7)	N21B-Ni2–S21	91.25(8)
N12–Ni1–S51	172.83(7)	N41–Ni2–S21	88.68(8)
N1–Ni1–S51	97.02(7)	N11–Ni2–S21	87.61(7)
O1–Ni1–S51	90.23(8)	N2–Ni2–S21	173.71(8)
C21B-N21B-Ni2	146.4(3)	C21–S21–Ni2	100.21(11)
C41–N41–Ni1	129.1(2)	C41–N41–Ni2	125.1(2)
Ni1–N41–Ni2	105.67(11)	C51A-N51A-Ni1	162.8(3)
C51–S51–Ni1	104.82(11)		

Symmetry codes: A = $-x + 1, -y + 2, -z$; B = $-x, -y + 1, -z + 1$.

Investigations on the Thermal Decomposition Reaction

On heating $[Ni(NCS)_2(pyridazine)(H_2O)_{0.5}]_n$ (**1I**) to 400 °C in a thermobalance, two mass steps are observed in the TG curve that are accompanied by endothermic events in the DTA curve. From the MS trend scan curve, it is proven that only water (m/z = 18) is emitted in the first mass step and pyridazine (m/z = 80) in the second. From the DTG curve it is obvious that these mass steps are well separated (Figure 4). The experimental mass losses of Δm_{exp}(1st step) = 3.3% and Δm_{exp}(2nd step) = 29.6% are in good agreement with that calculated for the loss of water and the pyridazine ligands, respectively [Δm_{calc}(water) = 3.4%, Δm_{calc}(pyridazine) = 30.3%].

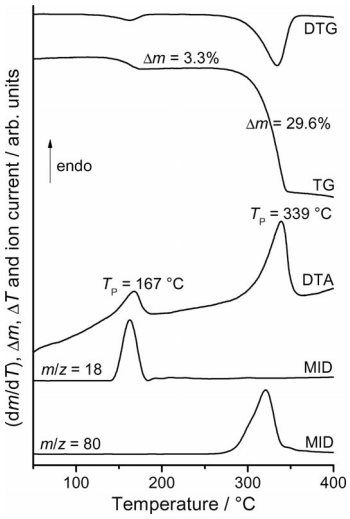

Figure 4. DTG, TG, DTA, and MS trend scan curves of compound **1I**. Heating rate: 4 °C min^{-1}; m/z = 18 (water) and 80 (pyridazine); the mass changes (%) and the peak temperatures T_P [°C] are given.

On the basis of the experimental mass losses, it can be assumed that in the first step the anhydrate $[Ni(NCS)_2(pyridazine)]_n$ (**2**) is formed, which loses the pyridazine ligands in the second step leading to the formation of $Ni(NCS)_2$.

To investigate the nature of the anhydrate **2** formed in the thermal decomposition reaction of the precursor compound **1I**, additional TG measurements were performed and stopped after the first TG step. The residue obtained was investigated by elemental analysis, X-ray powder diffraction, and infrared spectroscopy. The elemental analysis shows a composition that is in agreement with that calculated for an anhydrate ($C_6H_4N_4NiS_2$: calcd. C 28.27, H 1.58, N 21.98, S 25.16; found C 28.13, H 1.50, N 21.78, S 25.02). From XRPD investigations it is obvious that a low crystalline intermediate **2** is formed, which shows a completely different powder pattern from its precursor compound **1I** (see Figure S2, Supporting Information). Unfortunately, because of the extreme broadening of the reflection profiles, indexing of the powder pattern fails and therefore no structural information can be retrieved. But further structural information can be gained by IR spectroscopic data. In general it is well known that the value of the N–C stretching vibration for terminally *N*-bonded thiocyanates is found around 2100 cm^{-1},[3,16–18] for μ-1,3-NCS-bridging thiocyanates well above 2100 cm^{-1},[3,17–19] and for μ-1,1-NCS-bridging thiocyanates around 2000 cm^{-1}.[17,20,21] In agreement with the single-crystal data for **1I**, values of 1989, 2102, 2117, and 2129 cm^{-1} are found (see Figure S4, Supporting Information). The splitting of the latter bands is attributed to two independent μ-1,3-NCS bridges. For **2** values of 1989, 2098, 2126, and 2145 cm^{-1} are found, which clearly prove that terminally *N*-bonded and μ-1,1-NCS-bridging thiocyanato anions are still present (see Figure S5, Supporting Information). Because of the significant shifting of two bands it is obvious that some structural changes occurred, but no further information can be retrieved from

IR spectroscopic measurements alone. It must be noted that for **2** a broad OH stretching band around 3450 cm^{-1} is observed, which clearly shows that this compound is hygroscopic (see below).

Investigations on the Rehydration

To check the reversibility of the water removal a sample of the anhydrate **2** was stored for one day in a saturated water atmosphere. Thermogravimetry (see Figure S3, Supporting Information) and elemental analysis clearly show that a hemihydrate has been formed again, but investigations of this product by XRPD measurements surprisingly show a powder pattern that is different from that calculated for the precursor compound **1I** from single-crystal data (Figure 5). Obviously a new polymorphic modification was obtained, which according to additional IR spectroscopic investigations shows only very small differences in the characteristic frequencies (see Figure S6, Supporting Information). As for the anhydrate **2** no structural information was gained from X-ray powder investigations.

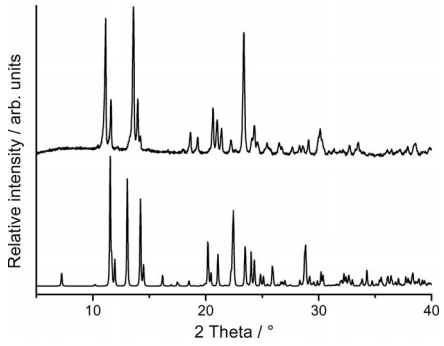

Figure 5. Experimental X-ray powder pattern of modification **1II** obtained by water removal from modification **1I** and following rehydration (top). Calculated powder pattern from single-crystal analysis of compound **1I** (bottom).

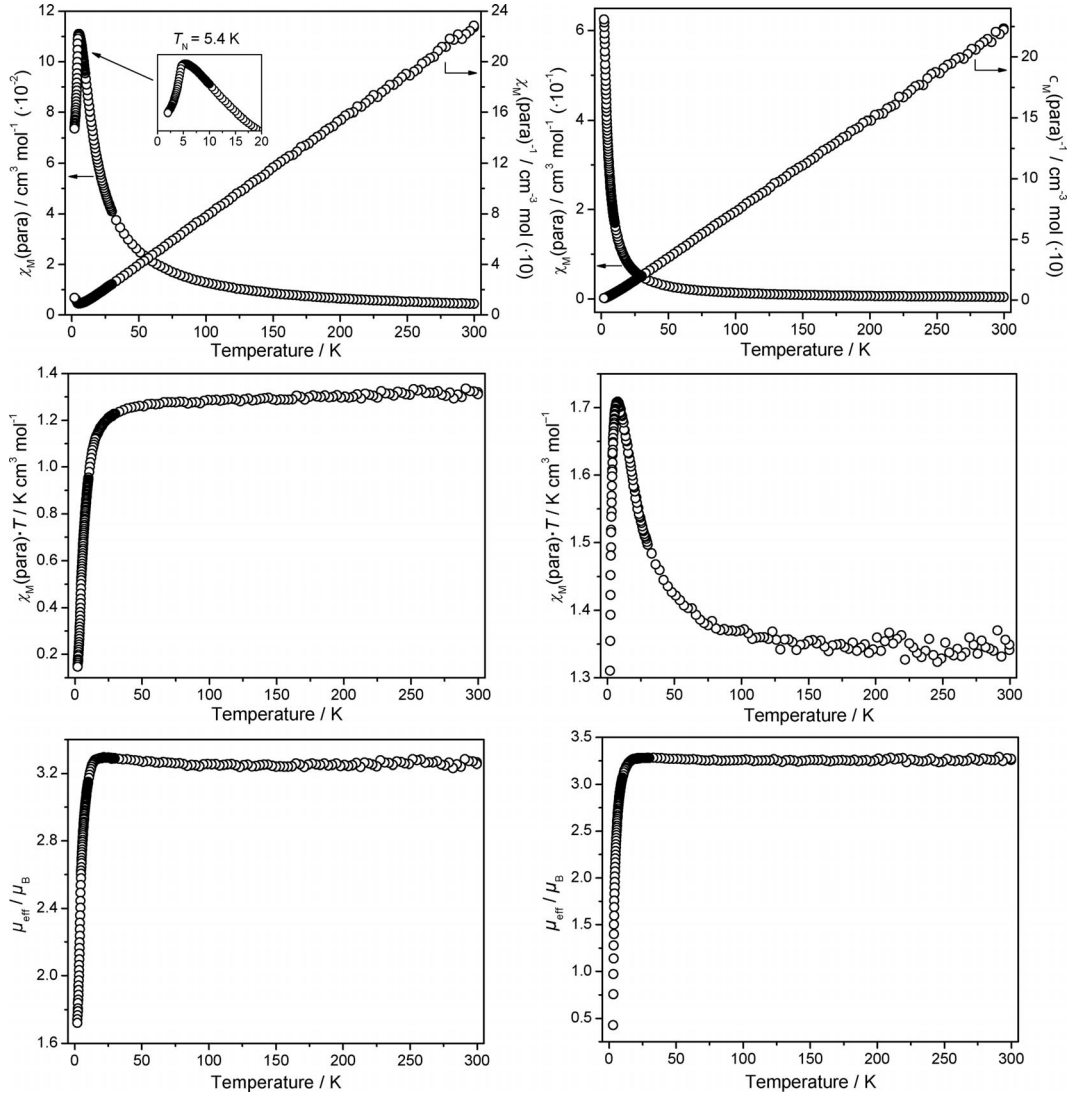

Figure 6. Results of the magnetic measurements for **1I** (left column) and **1II** (right column) from plots of the field-cooled paramagnetic susceptibility as a function of temperature (left side in the top graph), reciprocal paramagnetic susceptibility (right side in the top graph), $\chi_M T$ (middle), and the effective magnetic moment as a function of temperature (bottom), all at H = 0.1 T.

Magnetic Investigations

Both polymorphic modifications **1I** and **1II** as well as the anhydrate **2** were investigated for their magnetic properties. The temperature dependence of their susceptibility was investigated by applying a magnetic field of $H = 0.1$ T in the temperature range 300–2 K (Figure 6). However, detailed investigations on the stability of the anhydrate **2** by time-dependent X-ray powder diffraction measurements clearly prove that transformation into **1II** starts immediately at the beginning of the measurement. This is in agreement with additional XRPD investigations of the sample used for the magnetic measurements, which later show reflections of form **1II**. Thus no magnetic data for **2** can be presented.

Modification **1I** shows a sharp maximum in the χ_M vs. T curve, which indicates a long-range antiferromagnetic ordering at lower temperatures with $T_N = 5.4$ K. Above this ordering temperature the χ_M^{-1} vs. T curve is essentially linear following the Curie–Weiss law (Figure 6, top, left). The magnetic data between 20 to 300 K were fitted with the Curie–Weiss law $\chi_M = C/(T - \theta)$ yielding a negative Weiss constant $\theta = -3.0$ K, which confirms the antiferromagnetic behavior. The effective magnetic moment, μ_{eff}, of 3.26 μ_B is larger than the spin-only value of 2.83 μ_B for a high spin Ni^{II} ion ($S = 1$, $g = 2.00$), but it is well documented that a significant spin-orbit coupling/zero-field splitting with g values strongly deviating from 2.00 yields effective magnetic moments between 2.8 and 4.0 μ_B (Table 3).[22] The $\chi_M T$ values decrease constantly upon cooling, which further confirms the overall antiferromagnetic behavior (Figure 6, middle, left). The temperature dependence of the effective magnetic moment is consistent with the temperature dependence of the $\chi_M T$ values (Figure 6, bottom, left). It is well known that in nickel(II) compounds μ-1,2-pyridazine bridges mediate antiferromagnetic interactions,[8,21,23] whereas μ-1,3-NCS bridges mediate ferromagnetic interactions.[5,24] For μ-1,1-NCS-bridged nickel(II) compounds ferromagnetic[20,21,25] and antiferromagnetic[26] interactions are found. Thus, it can be assumed that the overall magnetic exchange pathway of the μ-1,2-pyridazine bridges must dominate.

Table 3. Results of the fits of the magnetic susceptibility data with the Curie–Weiss law for compounds **1I** and **1II**.

Compound	**1I**	**1II**
C [$cm^3 K mol^{-1}$]	1.33	1.33
θ [K]	–3.04	3.05
μ_{eff} (exp.) [μ_B]	3.26	3.26
μ_{eff} (calcd.)[22] [μ_B]	2.83	2.83
T_N [K]	5.4	–
Fit [K]	20–300	20–300

Surprisingly, modification **1II** shows only Curie–Weiss behavior, which is obvious from the χ_M vs. T curve and the linear χ_M^{-1} vs. T curve (Figure 6, top, right). The positive Weiss constant θ at 3.0 K indicates weak ferromagnetic exchange interactions (Table 3), which is consistent with increasing $\chi_M T$ values upon cooling to 8 K (Figure 6, middle, right). Below this temperature $\chi_M T$ values decrease rapidly, which might originate from dominating antiferromagnetic interactions of adjacent Ni^{II} centers. The average effective magnetic moment of 3.26 μ_B and its temperature dependence is equal to that of modification **1I** (see Table 3 and Figure 6, bottom, right). It can be assumed that the dominating antiferromagnetic interactions in **1I** mediated by the μ-1,2-pyridazine bridges are canceled by stronger ferromagnetic μ-1,3-NCS bridged interactions in **1II**. Therefore, only Curie–Weiss behavior with weak ferromagnetic interactions is observed.

Conclusion

In this contribution we have presented the new coordination polymer $[Ni(NCS)_2(pyridazine)(H_2O)_{0.5}]_n$ (**1I**), in which three different coordination modes of the thiocyanato anion (*N*-terminal, μ-1,1-NCS- and μ-1,3-NCS-bridging) are observed for the first time. All three modes can be clearly distinguished by IR spectroscopy. However, on heating compound **1I**, the anhydrate $[Ni(NCS)_2(pyridazine)]_n$ (**2**) is formed, which on rehydration leads to the formation of a new polymorphic hemihydrate modification **1II**. Magnetic measurements performed on form **1I** reveal that the antiferromagnetic interactions mediated by the μ-1,2-pyridazine bridges dominate the magnetic behavior and that a long-range antiferromagnetic ordering occurs on cooling with $T_N = 5.4$ K. In contrast, in form **1II** only Curie–Weiss behavior is observed, which indicates that the dominating antiferromagnetic interactions in **1I** are canceled by stronger ferromagnetic μ-1,3-NCS interactions in **1II**. Unfortunately, no detailed structural information on **1II** could be retrieved, but IR spectroscopic investigations strongly indicate that only minor structural changes occurred. These results clearly emphasize the importance of investigations on the polymorphism of coordination compounds, with a special focus on their differences in physical properties.

Experimental Section

Synthesis: $Ni(NCS)_2$ and pyridazine were obtained from Alfa Aesar and used without further purification.

Catena[bis(pyridazine-*N*,*N*′)aqua(isothiocyanato-*N*)bis(μ-1,3-thiocyanato-*N*,*S*)(μ-1,1-thiocyanato-*N*,*N*)dinickel(II)] (1I): $Ni(NCS)_2$ (87.4 mg, 0.5 mmol), pyridazine (20.0 mg, 0.25 mmol), and water (0.5 mL) were reacted in a closed test tube at 120 °C for 3 d while stirring. On cooling a green crystalline powder of **1I** was obtained. The residue was filtered off and washed with water and diethyl ether. The purity was checked by XRPD measurements (see Figure S1, Supporting Information). Yield based on pyridazine: 61.3 mg (92.9%). $C_6H_5N_4NiO_{0.5}S_2$ (263.95): calcd. C 27.30, H 1.91, N 21.23, S 24.30; found C 27.53, H 1.84, N 21.24, S 24.47. IR (KBr): $\tilde{\nu}$ = 3467 (br), 3070 (w), 2129 (s), 2117 (vs), 2102 (s), 1989 (vs), 1615 (m), 1580 (w), 1455 (w), 1413 (m), 1290 (w), 1073 (w), 993 (w), 763 (m), 674 (w), 547 (w), 470 (w) cm^{-1} (see Figure S4, Supporting Information).

Green block-shaped single crystals suitable for X-ray structure determination were obtained in the same way as that described above, but without stirring the reaction mixture.

Single-Crystal Structure Analysis: The crystal structure determination was performed with an imaging plate diffraction system (IPDS-1) with Mo-K_α-radiation from STOE & CIE. The structure solution was done with direct methods using SHELXS-97 and structure refinements were performed against $|F|^2$ using SHELXL-97.[27] A numerical absorption correction was applied using X-Red Version 1.31 and X-Shape Version 2.11 of the program package X-Area.[28] All non-hydrogen atoms were refined with anisotropic displacement parameters. All aromatic C–H hydrogen atoms were positioned with idealized geometries and were refined with fixed isotropic displacement parameters [U_{eq}(H) = –1.2·U_{eq}(C)] using a riding model with $d_{C–H}$ = 0.93 Å. The O–H hydrogen atoms were located in a difference map, their bond lengths were set to ideal values and finally they were refined using a riding model. Details of the structure determination are given in Table 4.

Table 4. Selected crystal data and details of the structure determination from single-crystal data.

Formula	$C_6H_5N_4NiO_{0.5}S_2$
M_r [g mol^{-1}]	263.95
Crystal system	triclinic
Space group	$P\bar{1}$
a [Å]	9.0913(6)
b [Å]	9.4529(6)
c [Å]	12.4989(7)
α [°]	90.617(5)
β [°]	100.867(5)
γ [°]	112.852(4)
V [Å^3]	967.89(10)
T [K]	293(2)
Z	4
$D_{calcd.}$ [g cm^{-3}]	1.811
μ [mm^{-1}]	2.397
Min./max. transmission	0.7234/0.8525
θ_{max} [°]	29.36
Measured reflections	12034
Unique reflections	5160
Reflections [$F_o > 4\sigma(F_o)$]	4151
Parameter	244
R_{int}	0.0372
R_1[a] [$F_o > 4\sigma(F_o)$]	0.0486
wR_2[b] [all data]	0.0769
Gof	1.180
$\Delta\rho_{max}$, $\Delta\rho_{min}$ [e Å^{-3}]	0.439, –0.592

[a] $R_1 = \sum||F_o| - |F_c||/\sum|F_o|$. [b] $wR_2 = \{\sum[w(F_o^2 - F_c^2)^2]/\sum[w(F_o^2)^2]\}^{1/2}$.

CCDC-790470 contains the supplementary crystallographic data for **1I**. The data can be obtained free of charge from the Cambridge Crystallographic Data Centre via http://www.ccdc.cam.ac.uk/.

X-ray Powder Diffraction (XRPD): XRPD experiments were performed using a PANalytical X'Pert Pro MPD Reflection Powder Diffraction System, with Cu-K_α radiation (λ = 154.0598 pm), that is equipped with a PIXcel semiconductor detector from PANalytical.

Differential Thermal Analysis, Thermogravimetry, and Mass Spectroscopy (DTA-TG-MS): The DTA-TG measurements were performed in a nitrogen atmosphere (purity: 5.0) in Al_2O_3 crucibles using a STA-409CD instrument from Netzsch. The DTA-TG-MS measurements were performed with the same instrument, which is connected to a quadrupole mass spectrometer from Balzers via Skimmer coupling from Netzsch. The MS measurements were performed in analogue and trend scan mode in Al_2O_3 crucibles in a dynamic nitrogen atmosphere (purity: 5.0) using heating rates of 4 °C min^{-1}. All measurements were performed with a flow rate of 75 mL min^{-1}. The instrument was calibrated using standard reference materials.

Elemental Analysis: CHNS analyses were performed using an EURO EA elemental analyzer, fabricated by EURO VECTOR Instruments and Software.

Spectroscopy: Fourier transform IR spectra were recorded with a Genesis series FTIR spectrometer, by ATI Mattson, using KBr pellets.

Magnetic Measurements: Magnetic measurements were performed using a physical property measuring system (PPMS) from Quantum Design, which is equipped with a 9 T magnet. The data were corrected for core diamagnetism.[29]

Supporting Information (see also the footnote on the first page of this article): Experimental and calculated XRPD data from single crystals of compound **1I**, comparison of the experimental XRPD data of compound **2** with that calculated for compound **1I**, IR data of all compounds.

Acknowledgments

This project was supported by the Deutsche Forschungsgemeinschaft (DFG) (project number NA 720/3-1) and the State of Schleswig-Holstein. M. W. thanks the Stiftung Stipendien-Fonds des Verbandes der Chemischen Industrie and the Studienstiftung des deutschen Volkes for a PhD scholarship. We thank Professor Dr. Wolfgang Bensch for the opportunity to use his experimental facility. Special thanks go to Inke Jeß for her support with the single-crystal measurements and to Sina Sellmer for his experimental support.

[1] a) D. Braga, L. Maini, M. Polito, L. Scaccianoce, G. Cojazzi, F. Grepioni, *Coord. Chem. Rev.* **2001**, *216*, 225–248; b) P. J. Hagrman, D. Hagrman, J. Zubieta, *Angew. Chem. Int. Ed.* **1999**, *38*, 2638–2684; c) S. L. James, *Chem. Soc. Rev.* **2003**, *32*, 276–288; d) C. Janiak, *Dalton Trans.* **2003**, 2781–2804; e) A. N. Khlobystov, A. J. Blake, N. R. Champness, D. A. Lemenovskii, A. G. Majouga, N. V. Zyk, M. Schröder, *Coord. Chem. Rev.* **2001**, *222*, 155–192; f) S. Kitagawa, R. Matsuda, *Coord. Chem. Rev.* **2007**, *251*, 2490–2509; g) S. Kitagawa, K. Uemura, *Chem. Soc. Rev.* **2005**, *34*, 109–119; h) D. Maspoch, D. Ruiz-Molina, J. Veciana, *Chem. Soc. Rev.* **2007**, *36*, 770–818; i) R. J. Puddephatt, *Coord. Chem. Rev.* **2001**, *216–217*, 313–332; j) A. Y. Robin, K. M. Fromm, *Coord. Chem. Rev.* **2006**, *250*, 2127–2157.

[2] a) K. S. Gavrilenko, O. Cador, K. Bernot, P. Rosa, R. Sessoli, S. Golhen, V. V. Pavlishchuk, L. Ouahab, *Chem. Eur. J.* **2008**, *14*, 2034–2043; b) J. S. Miller, A. J. Epstein, *Angew. Chem.* **1994**, *106*, 399–432; c) W. Li, H.-P. Jia, Z.-F. Ju, J. Zhang, *Dalton Trans.* **2008**, 5350–5357; d) H. Miyasaka, M. Yamashita, *Dalton Trans.* **2007**, 399–406; e) E. Pardo, R. Ruiz-Garcia, J. Cano, X. Ottenwaelder, R. Lescouezec, Y. Journaux, F. Lloret, M. Julve, *Dalton Trans.* **2008**, 2780–2805; f) A. Prescimone, J. Wolowska, G. Rajaraman, S. Parsons, W. Wernsdorfer, M. Murugesu, G. Christou, S. Piligkos, E. J. L. McInnes, E. K. Brechin, *Dalton Trans.* **2007**, 5282–5289; g) L. M. Toma, R. Lescouezec, J. Pasan, C. Ruiz-Perez, J. Vaissermann, J. Cano, R. Carrasco, W. Wernsdorfer, F. Lloret, M. Julve, *J. Am. Chem. Soc.* **2006**, *128*, 4842–4853; h) M. Verdaguer, A. Bleuzen, C. Train, R. Garde, F. F. d. Biani, C. Desplanches, *Phil. Trans. R. Soc. London Ser. A* **1999**, *357*, 2959–2976.

[3] M. G. Barandika, M. L. Hernandez-Pino, M. K. Urtiaga, R. Cortes, L. Lezama, M. I. Arriortua, T. Rojo, *J. Chem. Soc., Dalton Trans.* **2000**, *9*, 1469–1473.

[4] a) H. N. Bordallo, L. Chapon, J. L. Manson, C. D. Ling, J. S. Qualls, D. Hall, D. N. Argyriou, *Polyhedron* **2003**, *22*, 2045–2049; b) M. Julve, M. Verdaguer, G. Demunno, J. A. Real, G.

Bruno, *Inorg. Chem.* **1993**, *32*, 795–802; c) R. Vicente, A. Escuer, E. Penalba, X. Solans, M. FontBardia, *Inorg. Chim. Acta* **1997**, *255*, 7–12.
[5] a) M. Monfort, C. Bastos, C. Diaz, J. Ribas, X. Solans, *Inorg. Chim. Acta* **1994**, *218*, 185–188; b) M. Monfort, J. Ribas, X. Solans, *Inorg. Chem.* **1994**, *33*, 4271–4276; c) T. Rojo, R. Cortes, L. Lezama, M. I. Arriortua, K. Urtiaga, G. Villeneuve, *J. Chem. Soc., Dalton Trans.* **1991**, 1779–1783; d) R. Vicente, A. Escuer, J. Ribas, X. Solans, *J. Chem. Soc., Dalton Trans.* **1994**, 259–262.
[6] a) M. Wriedt, I. Jeß, C. Näther, *Eur. J. Inorg. Chem.* **2009**, 1406–1413; b) C. Näther, J. Greve, *J. Solid State Chem.* **2003**, *176*, 259–265.
[7] a) M. Wriedt, C. Näther, *Z. Anorg. Allg. Chem.* **2009**, *636*, 569–575; b) M. Wriedt, C. Näther, *Dalton Trans.* **2009**, 10192–10198; c) M. Wriedt, S. Sellmer, C. Näther, *Inorg. Chem.* **2009**, *48*, 6896–6903.
[8] M. Wriedt, C. Näther, *Z. Anorg. Allg. Chem.* **2009**, *635*, 2459–2464.
[9] M. Wriedt, S. Sellmer, C. Näther, *Dalton Trans.* **2009**, 7975–7984.
[10] M. Wriedt, C. Näther, *Eur. J. Inorg. Chem.* **2010**, 3201–3211.
[11] M. Wriedt, C. Näther, *Z. Anorg. Allg. Chem.* **2010**, *636*, 1061–1068.
[12] M. Wriedt, C. Näther, *Chem. Commun.* **2010**, *46*, 4707–4709.
[13] J. Boeckmann, M. Wriedt, C. Näther, *Eur. J. Inorg. Chem.* **2010**, 1820–1828.
[14] M. Wriedt, C. Näther, *Dalton Trans.* **2010**, in press.
[15] C. Näther, J. Greve, I. Jeß, *Chem. Mater.* **2002**, *14*, 4536–4542; J. Greve, I. Jeß, C. Näther, *J. Solid State Chem.* **2003**, *175*, 328–340.
[16] R. A. Bailey, S. L. Kozak, T. W. Michelsen, W. N. Mills, *Coord. Chem. Rev.* **1971**, *6*, 407–445.
[17] L. Shen, Y.-Z. Xu, *J. Chem. Soc., Dalton Trans.* **2001**, 3413–3414.
[18] J. S. Haynes, A. Kostikas, J. R. Sams, A. Simopoulos, R. C. Thompson, *Inorg. Chem.* **1987**, *26*, 2630–2637.
[19] L. Yi, B. Ding, B. Zhao, P. Cheng, D.-Z. Liao, S.-P. Yan, Z.-H. Jiang, *Inorg. Chem.* **2004**, *43*, 33–43.
[20] G. A. V. Albada, R. A. G. D. Graaff, J. G. Haasnoot, J. Reedijk, *Inorg. Chem.* **1984**, *23*, 1404–1408.
[21] J. Cano, G. D. Munno, F. Lloret, M. Julve, *Inorg. Chem.* **2000**, *39*, 1611–1614.
[22] A. F. Holleman, E. Wiberg, *Lehrbuch der Anorganischen Chemie*, vol. 101, de Gruyter, Berlin, New York, **1995**.
[23] a) T. Yi, C. Ho-Chol, S. Gao, S. Kitagawa, *Eur. J. Inorg. Chem.* **2006**, 1381–1387; b) A. Escuer, R. Vicente, B. Mernari, A. El Gueddi, M. Pierrot, *Inorg. Chem.* **1997**, *36*, 2511–2516.
[24] a) D. M. Duggan, D. N. Hendrickson, *Inorg. Chem.* **1974**, *13*, 2929–2940; b) T. K. Maji, I. R. Laskar, G. Mostafa, A. J. Welch, P. S. Mukherjee, N. R. Chaudhuri, *Polyhedron* **2001**, *20*, 651–655; c) H.-D. Bian, W. Gu, Q. Yu, S.-P. Yan, D.-Z. Liao, Z.-H. Jiang, P. Cheng, *Polyhedron* **2005**, *24*, 2002–2008; d) X.-T. Liu, Y.-S. Xie, Q.-L. Liu, *Synth. React. Inorg. Met.-Org. Chem.* **2007**, *37*, 301–305; e) H.-Z. Kou, S. Hishiya, O. Sato, *Inorg. Chim. Acta* **2008**, *361*, 2396–2406.
[25] Q. Zhao, H. Li, Z. Chen, R. Fang, *Inorg. Chim. Acta* **2002**, *336*, 142–146.
[26] R. Kapoor, A. Kataria, A. Pathak, P. Venugopalan, G. Hundal, P. Kapoor, *Polyhedron* **2005**, *24*, 1221–1231.
[27] G. M. Sheldrick, *Acta Crystallogr., Sect. A* **2008**, *64*, 112–122.
[28] *X-Area*, version 1.44, *Program Package for Single Crystal Measurements*, STOE & CIE GmbH, Darmstadt, Germany, **2008**.
[29] G. A. Bain, J. F. Berry, *J. Chem. Educ.* **2008**, *85*, 532–536.

Received: August 6, 2010
Published Online: November 25, 2010

